Accelerated Oxygen Atom Transfer and C–H Bond Oxygenation by Remote Redox Changes in Fe₃Mn-Iodosobenzene Adducts

Dr. Graham de Ruiter+,

Department of Chemistry and Chemical Engineering California Institute of Technology; MC 127-72 Pasadena, CA 91125 (USA)

Kurtis M. Carsch+,

Department of Chemistry and Chemical Engineering California Institute of Technology; MC 127-72 Pasadena, CA 91125 (USA)

Dr. Sheraz Gul,

Molecular Biophysics & Integrated Bioimaging Division Lawrence Berkeley National Laboratory Berkeley, CA 94720 (USA)

Dr. Ruchira Chatterjee,

Molecular Biophysics & Integrated Bioimaging Division Lawrence Berkeley National Laboratory Berkeley, CA 94720 (USA)

Niklas B. Thompson,

Department of Chemistry and Chemical Engineering California Institute of Technology; MC 127-72 Pasadena, CA 91125 (USA)

Dr. Michael K. Takase,

Department of Chemistry and Chemical Engineering California Institute of Technology; MC 127-72 Pasadena, CA 91125 (USA)

Dr. Junko Yano, and

Molecular Biophysics & Integrated Bioimaging Division Lawrence Berkeley National Laboratory Berkeley, CA 94720 (USA)

Prof. Theodor Agapie

Department of Chemistry and Chemical Engineering California Institute of Technology; MC 127-72 Pasadena, CA 91125 (USA)

Abstract

We report the synthesis, characterization, and reactivity of $[LFe_3(PhPz)_3OMn(^SPhIO)][OTf]_x$ (**3**: x = 2; **4**: x = 3), where **4** is one of very few examples of iodosobenzene–metal adducts characterized by X-ray crystallography. Access to these rare heterometallic clusters enabled differentiation of the

Correspondence to: Theodor Agapie.

[+] These authors contributed equally to this work.

Conflict of interest

The authors declare no conflict of interest.

metal centers involved in oxygen atom transfer (Mn) or redox modulation (Fe). Specifically, [57]Fe Mössbauer and X-ray absorption spectroscopy provided unique insights into how changes in oxidation state ($\mathbf{Fe^{III}_2Fe^{II}Mn^{II}}$ vs. $\mathbf{Fe^{III}_3Mn^{II}}$) influence oxygen atom transfer in tetranuclear Fe_3Mn clusters. In particular, a one-electron redox change at a distal metal site leads to a change in oxygen atom transfer reactivity by ca. two orders of magnitude.

Keywords

C–H bond oxygenation; clusters; iodosobenzene adduct; multimetallic complexes; oxygen atom transfer

---

Terminal metal-oxo moieties are commonly invoked in oxidative biological transformations.[1] Due to the important functions of reactive metal-oxo motifs in C–H bond functionalization and water oxidation, intense efforts have been made to develop synthetic model complexes to elucidate their behavior through structure–function studies.[2] Both the oxidation- and spin-state of the metal center affect their reactivity.[3] Nonetheless, studying these effects on C–H bond activation or oxygen atom transfer is challenging due to limitations in accessing metal complexes with properties suitable for meaningful comparison.[2d,4] Such studies are even more challenging in multinuclear systems, which represent more accurate models of enzymes' active sites.[1f,5] Only recently, a study of bimetallic complexes demonstrated that changing the oxidation state from [HO-Fe^{IV}-O-Fe^{IV}=O] to [HO-Fe^{III}-O-Fe^{IV}=O] resulted in a change in spin-state, concomitant with a remarkable million-fold increase in the rate of C–H bond cleavage.[6] Apart from bimetallic complexes, there are no other reports, to our knowledge, that examine the effect of remote redox changes on oxygen atom transfer (OAT) or C–H bond oxygenation.

Herein, we report on the synthesis and characterization of a new series of clusters, [LFe$_3$(PhPz)$_3$OMn][OTf]$_x$ (Figure 1; **1**: $x = 2$; **2**: $x = 3$), and demonstrate how changing the oxidation state ($\mathbf{Fe^{III}_2Fe^{II}Mn^{II}}$ vs. $\mathbf{Fe^{III}_3Mn^{II}}$) has profound effects on the rate of oxygen atom transfer from their corresponding iodosobenzene adducts [LFe$_3$(PhPz)$_3$OMn(^{s}PhIO)][OTf]$_x$ (**3**: $x = 2$; and **4**: $x = 3$). Compound **4** is stable for a few hours at room temperature (RT), and constitutes one of the very rare example of a iodosobenzene adduct characterized by X-ray crystallography.[7] Access to these heterometallic clusters enabled us to differentiate the Mn and Fe metal centers by both [57]Fe Mössbauer and X-ray absorption spectroscopy (XAS), giving unique insights into the structure and reactivity of **3** and **4** where coordination of iodosobenzene to low-valent Mn^{II} is observed.

Complexes [LFe$_3$(PhPz)$_3$OMn][OTf]$_2$ (**1**) and [LFe$_3$(PhPz)$_3$OMn][OTf]$_3$ (**2**; PhPz = phenylpyrazolate, OTf = trifluoromethanesulfonate) were prepared by modifying our recently reported literature procedure for [LFe$_3$(PhPz)$_3$OFe][OTf]$_2$.[8] Both **1** and **2** were fully characterized by a wide variety of physical methods including ^{1}H NMR spectroscopy (Figures S1 and S2 in the Supporting Information), X-ray crystallography (Figure 2, and Figures S20 and S21), Mössbauer spectroscopy (Figure S17), and X-ray absorption spectroscopy (Figures S12–S14).

Access to different oxidation states ($\mathbf{Fe^{III}_2Fe^{II}Mn^{II}}$ vs. $\mathbf{Fe^{III}_3Mn^{II}}$) in complexes **1** and **2** allows for structure–reactivity studies. Given the function of the multinuclear oxygen evolving complex (OEC) in water oxidation and of diiron active sites in C–H oxygenation chemistry, O-atom transfer was studied by treatment of **1** and **2** with 2-(*tert*-butylsulfonyl)-iodosobenzene (^{s}PhIO; 5.0 equiv). Indeed, en route towards intramolecular C–H bond oxygenation,[9] distinct intermediates (**3**, **4**) were observed by ^{1}H NMR spectroscopy (Figures S3 and S4), where **4** exhibits diminished reactivity. No other intermediates were observed prior to the formation of [LFe$_3$(PhPz)$_2$(OArPz)OMn][OTf]$_x$ (Scheme 1. **5**: $x = 2$; **6**: $x = 3$).[10] Intrigued by the formation of **3** and **4**, their structure and reactivity were further investigated by various analytical methods, where the relative stability of **4** enabled us to isolate crystals amenable for X-ray crystallography.

X-ray diffraction (XRD) studies on single crystals of **4** (Figure 2C), revealed the formation of a rare isolable iodosobenzene adduct [LFe$_3$(PhPz)$_3$OMn(^{s}PhIO)][OTf]$_3$. Comparing the O2–I1 (1.848(6) Å) and I1–C101 (2.128(7) Å) bond distances in **4** (Figure 2C), to those observed for free ^{s}PhIO (1.864(10) and 2.105(15) Å)[11] reveals no significant ^{s}PhIO activation (Table S1). This lack of activation is further corroborated by comparing the Mn1–O1 bond distances in complex **2** (2.166(3) Å) to those in **4** (2.100(6) Å). The long distances indicate that even upon binding of sPhIO, the manganese metal center remains Mn^{II}.[12] Subsequent XAS studies confirm such an assignment (see below).

The isolation of an iodosobenzene adduct bound to a low-valent Mn^{II} metal center is unique. To date, only two other examples are known where iodosobenzene is bound to a biologically relevant metal (Mn or Fe),[7b,c] none of them being on a multimetallic scaffold. Furthermore, in both complexes, the iodosobenzene is bound to higher oxidation state metal centers (Fe^{III} and Mn^{IV}), which are less prone to further oxidation and feature larger degrees of PhIO activation. These differences suggest a multimetallic effect where the distal metal centers affect the reactivity of the Mn^{II} that ligates iodosobenzene.

To gain further insight into the reactivity and oxidation state assignment of **3** and **4**, their properties were investigated by X-ray absorption spectroscopy (XAS). XAS is an element-specific technique that provides information about the oxidation state and local coordination environment of metal ions.[13] The Mn K-edge X-ray absorption near edge structure (XANES) spectra for complexes **3** and **4** are nearly identical, with rising edge energies (at half-height of the absorption edge) of 6547.8 eV (**3**) and 6547.7 eV (**4**) respectively (Figure 3; dashed green and red traces). These values are close to that recorded for MnO (6546.4 eV; Figure 3; dotted brown trace), and slightly lower than that recorded for mixed-valent Mn$_3$O$_4$ (6548.9 eV; Figure 3; dotted black trace). For comparison, the XANES spectra for **5** and **6** are clearly at a higher energy, where the rising edge energies obtained for **5** (6550.7 eV) and **6** (6550.9 eV) are close to that of Mn$_2^{III}$O$_3$(6550.7 eV), suggesting the presence of higher oxidation state metal centers (Figure 3; solid green and red traces). The short Mn1–O1 (**5**: 1.894(7) Å; **6**: 1.943(4) Å) and Mn1–O2 (**5**:1.854(7) Å; **6**: 1.819(9) Å) bond distances support such an assignment (Figure 2B, Figure S24, Table S1).[14] The Mn XANES data thus indicate that prior to C–H bond oxygenation a lower oxidation state (Mn^{II}) metal center is present in **3** and **4**, which oxidizes (to Mn^{III}) along the reaction pathway. Moreover, the comparable shapes of the XAS spectra for **3** and **4** suggest a similar coordination geometry

around the Mn metal center.[13] Based on these data, we propose that **3** is also an iodosobenzene adduct. The agreement between the Mn K-edge extended X-ray absorption fine structure (EXAFS) derived bond distances in **3** (Mn–O_{avg}: 2.03 ± 0.02 Å; Mn–N_{avg}: 2.18±0.03 Å) with those obtained by XRD in **4** (Mn–O_{avg}: 2.07±0.03 Å; Mn–N_{avg}: 2.17±0.01 Å), supports such a proposal (Tables S4 and S5).[15]

The Fe K-edge XAS is very useful for establishing the iron oxidation states in **3**, for which no Mössbauer or XRD data is available. The Fe K-edge XANES of **3** (Figure 3, dashed green trace) is in between that of Fe_2O_3 (Fe^{III}; dotted gray trace) and $FeCl_2$ (Fe^{II}; dotted black trace). The closer proximity of the rising edge energy in **3** (7122.2 eV) to that of Fe_2O_3 (7123.3 eV), indicates that the triiron core is of mixed valence and mainly Fe^{III} in character. Moreover, the rising edge energy in **3** is nearly identical to that of **5** (7121.9 eV), for which a [$Fe^{II}Fe^{III}_2$] oxidation state was established by Mössbauer spectroscopy and X-ray crystallography (Figures S19 and S23). The XAS data therefore indicates an overall [$LFe^{III}_2Fe^{II}(PhPz)_3OMn^{II}(^sPhIO)$][OTf]$_2$ assignment for complex **3**.

Analogous to **3**, the Fe XANES spectrum of **4** is nearly identical to that of **6**, suggesting the same oxidation state of the triiron core (Figure 3; dashed and solid red traces). The rising edge energies of 7123.8 eV (**4**) and 7123.5 eV (**6**) are very similar to that of Fe_2O_3 (7123.4 eV) suggesting an [Fe^{III}_3] assignment for the triiron core. The short Fe_{core}–O1 distances of 1.994(7) Å (Fe1–O1), 1.989(7) Å (Fe2–O1), and 1.967(6) Å (Fe3–O1), are in line with such an assignment (Table S1).[16] The overall oxidation state in **4** is thus assigned as [$LFe^{III}_3(PhPz)_3OMn^{II}(^sPhIO)$][OTf]$_3$ based on X-ray crystallography and XAS spectroscopy.

The presence of an [Fe^{III}_3] triiron core in **4** was further supported by Mössbauer spectroscopy (Figure 4). The Mössbauer spectrum was modeled as three nearly identical quadrupole doublets in a 1:1:1 ratio with isomer shifts of $\delta = 0.42$ mms^{-1} (| E_Q|= 0.76 mms^{-1}), $\delta = 0.46$ mms^{-1} (| E_Q|= 0.92 mms^{-1}), and $\delta = 0.47$ mms^{-1} (| E_Q|= 0.71), consistent with the presence of three high spin ferric ions. The fitted parameters are similar to previously reported triiron oxo/hydroxo clusters.[16] Comparing the Mössbauer parameters of complexes **1**, **2**, and **4–6** (Figures S17–S19; Table S8), to our previously reported complexes [Fe$_3$(PhPz)$_3$OFe][OTf]$_x$ and [Fe$_3$(PhPz)$_2$(OArPz)OFe][OTf]$_x$ ($x = 2$–3) reveals a notable difference: the quadrupole doublet at $\delta \approx 0.86$ mms^{-1} (| E_Q| ≈ 1.57 mms^{-1}), associated with the apical iron metal center, is absent in our Mössbauer spectra.[8,9] The absence is significant and implies that no metal scrambling occurs within our [LFe$_3$(PhPz)$_3$OMn][OTf]$_x$ ($x = 2$–3) clusters, confirming that reactivity originates from the Mn metal center.

Overall, prior to C–H bond oxygenation, XRD, XAS, and Mössbauer spectroscopy provide conclusive evidence for assigning **3** and **4** as iodosobenzene adducts [LFe$_3$(PhPz)$_3$OMn(^sPhIO)][OTf]$_x$ (**3**: $x = 2$; **4**: $x = 3$) in which a low-valent Mn^{II} metal center engages in the interaction with iodosobenzene. Accessing these intermediates offers a unique opportunity to study the effect of remote redox changes (**Fe$^{III}_2$Fe^{II}Mn^{II}** vs. **Fe$^{III}_3$Mn^{II}**) on oxygen atom transfer. Indeed, pronounced redox state effects in **3** and **4** were observed. Warming a solution of **3** from −78°C to RT resulted—within two minutes—in the

quantitative conversion to the C–H bond oxygenated product **5** (Scheme 1; Figure S9). In contrast, compound **4** persists for at least three hours (> 200 min) at RT; during which a gradual conversion to complex **6** occurs (Scheme 1; Figure S10). A difference of at least two orders of magnitude is observed for oxygen atom transfer in complexes **3** and **4**.

The difference in reactivity between **3** and **4** is notable given that the XAS and XRD data (vide supra) suggest a similar degree of ^{s}PhIO activation. Assuming that ^{s}PhIO binds to the cluster as a neutral ligand, we propose that the redox properties of **3** and **4** should be comparable to their parent complexes **1** and **2**.[8] Based on this assumption, we suggest that the reactivity differences between **3** and **4** are due to the higher oxidative stability of **4**. The cyclic voltammogram of **1** is shown in Figure S11 and indeed reveals that the oxidation potential of **2** ($Fe^{III}_3Mn^{II}$) is at least 500 mV more positive than that of **1** ($Fe^{III}_2Fe^{II}Mn^{II}$).[17] The increased oxidative stability of **2** results in a slower oxygen atom transfer reaction; prolonging the lifetime of **4**, and hence, resulting in a more sluggish overall C–H oxygenation reaction.[18] Other effects such as spin-state changes, intramolecular electron transfer, or differences in the interaction with ancillary ligands cannot be ruled out. Nonetheless, these studies demonstrate a significant effect on reactivity where redox state changes at remote metal centers influence bond cleavage and formation at a distant Mn metal center. The observed differences suggest a path for the mechanism of C–H bond oxygenation. One can envision that the direct electrophilic attack or hydrogen atom abstraction from **3** or **4** would favor the metal complex with the highest oxidation potential.[19] However, here the opposite trend is observed, and is more consistent with the formation of a putative terminal Mn^{IV}-oxo, which if rate-limiting, is expected to be slower for the more oxidized metal cluster **4** compared to **3**.

In summary, rare examples of iodosobenzene adducts [LFe$_3$(PhPz)$_3$OMn(sPhIO)][OTf]$_x$. (**3**: $x = 2$; **4**: $x = 3$) were characterized by a variety of spectroscopic methods. The first example of structurally characterized iodosobenzene adduct to a low oxidation state (Mn^{II}) metal center was reported. The oxidation states of a remote triiron core (**$Fe^{III}_2Fe^{II}Mn^{II}$** vs. **$Fe^{III}_3Mn^{II}$**) was found to affect significantly oxygen atom transfer at a single manganese (Mn^{II}) metal center, and the overall C–H oxygenation chemistry in this system. These investigations provide a demonstration of the significant reactivity differences engendered by changes in the redox states of clusters, even at positions distant from where bond activations occur.

Supplementary Material

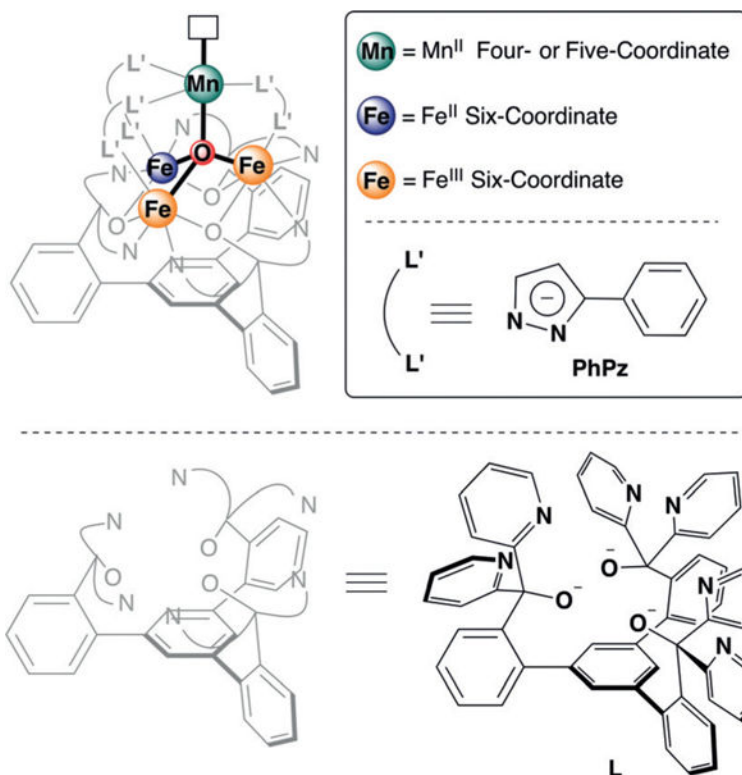Refer to Web version on PubMed Central for supplementary material.

Acknowledgments

References

1. a) Rittle J, Green MT. Science. 2010; 330:933–937. [PubMed: 21071661] b) Price JC, Barr EW, Tirupati B, Bollinger JM, Krebs C. Biochemistry. 2003; 42:7497–7508. [PubMed: 12809506] c) McDonald AR, Que L Jr. Coord Chem Rev. 2013; 257:414–428.d) Krebs C, Galoni Fujimori D, Walsh CT, Bollinger JM. Acc Chem Res. 2007; 40:484–492. [PubMed: 17542550] e) Costas M, Mehn MP, Jensen MP, Que L. Chem Rev. 2004; 104:939–986. [PubMed: 14871146] f) Yano J, Yachandra V. Chem Rev. 2014; 114:4175–4205. [PubMed: 24684576]

2. a) Park YJ, Matson EM, Nilges MJ, Fout AR. Chem Commun. 2015; 51:5310–5313.b) Sahu S, Widger LR, Quesne MG, de Visser SP, Matsumura H, Moënne-Loccoz P, Siegler MA, Goldberg DP. J Am Chem Soc. 2013; 135:10590–10593. [PubMed: 23834409] c) Taguchi T, Gupta R, Lassalle-Kaiser B, Boyce DW, Yachandra VK, Tolman WB, Yano J, Hendrich MP, Borovik AS. J Am Chem Soc. 2012; 134:1996–1999. [PubMed: 22233169] d) Parsell TH, Yang MY, Borovik AS. J Am Chem Soc. 2009; 131:2762–2763. [PubMed: 19196005] e) McGown AJ, Kerber WD, Fujii H, Goldberg DP. J Am Chem Soc. 2009; 131:8040–8048. [PubMed: 19462977] f) Lansky DE, Goldberg DP. Inorg Chem. 2006; 45:5119–5125. [PubMed: 16780334] g) Rohde J-U, In J-H, Lim MH, Brennessel WW, Bukowski MR, Stubna A, Münck E, Nam W, Que L. Science. 2003; 299:1037–1039. [PubMed: 12586936] h) MacBeth CE, Golombek AP, Young VG, Yang C, Kuczera K, Hendrich MP, Borovik AS. Science. 2000; 289:938–941. [PubMed: 10937994] i) Gross Z, Golubkov G, Simkhovich L. Angew Chem Int Ed. 2000; 39:4045–4047.Angew Chem. 2000; 112:4211–4213.j) Charnock JM, Garner CD, Trautwein AX, Bill E, Winkler H, Ayougou K, Mandon D, Weiss R. Angew Chem Int Ed Engl. 1995; 34:343–346.Angew Chem. 1995; 107:370–373.k) Groves JT, Stern MK. J Am Chem Soc. 1988; 110:8628–8638.l) Groves JT, Haushalter RC, Nakamura M, Nemo TE, Evans BJ. J Am Chem Soc. 1981; 103:2884–2886.m) Cook SA, Borovik AS. Acc Chem Res. 2015; 48:2407–2414. [PubMed: 26181849] n) Puri M, Que L. Acc Chem Res. 2015; 48:2443–2452. [PubMed: 26176555] o) Nam W. Acc Chem Res. 2015; 48:2415–2423. [PubMed: 26203519] p) Hohenberger J, Ray K, Meyer K. Nat Commun. 2012; 3:720. [PubMed: 22395611] q) Borovik AS. Chem Soc Rev. 2011; 40:1870–1874. [PubMed: 21365079]

3. a) Swart, M., Costas, M. Spin States in Biochemistry and Inorganic Chemistry. Wiley; Weinheim: 2015. b) Usharani D, Janardanan D, Li C, Shaik S. Acc Chem Res. 2013; 46:471–482. [PubMed: 23210564] c) Latifi R, Tahsini L, Karamzadeh B, Safari N, Nam W, de Visser SP. Arch Biochem Biophys. 2011; 507:4–13. [PubMed: 21216220] d) Hirao H, Kumar D, Que L, Shaik S. J Am Chem Soc. 2006; 128:8590–8606. [PubMed: 16802826]

4. a) Yang T, Quesne MG, Neu HM, Cantffl Reinhard FG, Goldberg DP, de Visser SP. J Am Chem Soc. 2016; 138:12375–12386. [PubMed: 27545752] b) Boaz NC, Bell SR, Groves JT. J Am Chem Soc. 2015; 137:2875–2885. [PubMed: 25651467] c) Usharani D, Lacy DC, Borovik AS, Shaik S. J Am Chem Soc. 2013; 135:17090–17104. [PubMed: 24124906] d) Prokop KA, Neu HM, de Visser SP, Goldberg DP. J Am Chem Soc. 2011; 133:15874–15877. [PubMed: 21888343] e) Arunkumar C, Lee YM, Lee JY, Fukuzumi S, Nam W. Chem Eur J. 2009; 15:11482–11489. [PubMed: 19810056]

5. Tsui EY, Kanady JS, Agapie T. Inorg Chem. 2013; 52:13833–13848. [PubMed: 24328344]

6. Xue G, De Hont R, Münck E, Que L. Nat Chem. 2010; 2:400–405. [PubMed: 20414242]

7. A comprehensive CSD search (Feb 2017), revealed only three structures with a M···O···I···C motif:a) Turlington CR, Morris J, White PS, Brennessel WW, Jones WD, Brookhart M, Templeton JL. Organometallics. 2014; 33:4442–4448.b) Wang C, Kurahashi T, Fujii H. Angew Chem Int Ed. 2012; 51:7809–7811.Angew Chem. 2012; 124:7929–7931.c) Lennartson A, McKenzie CJ. Angew Chem Int Ed. 2012; 51:6767–6770.Angew Chem. 2012; 124:6871–6874.

8. de Ruiter G, Thompson NB, Lionetti D, Agapie T. J Am Chem Soc. 2015; 137:14094–14106. [PubMed: 26390375]

9. de Ruiter G, Thompson NB, Takase MK, Agapie T. J Am Chem Soc. 2016; 138:1486–1489. [PubMed: 26760217]

10. The formation of $[LFe_3(PhPz)_2(OArPz)OMn][OTf]_x$ (x = 2 or 3) proceeds with the formal loss of a H-atom. Similar reactivity has been observed in isostructural Fe4 complexes. See:de Ruiter G, Thompson NB, Takase MK, Agapie T. J Am Chem Soc. 2016; 138:1486–1489. [PubMed: 26760217]

11. Macikenas D, Skrzypczak-Jankun E, Protasiewicz JD. Angew Chem Int Ed. 2000; 39:2007–2010.Angew Chem. 2000; 112:2063–2066.

12. a) Cotton FA, Daniels LM, Jordan GT IV, Murillo CA, Pascual I. Inorg Chim Acta. 2000; 297:6–10.b) McKee V, Tandon SS. J Chem Soc Chem Commun. 1988:1334–1336.

13. Yano J, Yachandra VK. Photosynth Res. 2009; 102:241. [PubMed: 19653117]

14. a) Nesterova OV, Chygorin EN, Kokozay VN, Omelchenko IV, Shishkin OV, Boca R, Pombeiro AJL. Dalton Trans. 2015; 44:14918–14924. [PubMed: 26225546] b) Milios CJ, Piligkos S, Bell AR, Laye RH, Teat SJ, Vicente R, McInnes E, Escuer A, Perlepes SP, Winpenny REP. Inorg Chem Commun. 2006; 9:638–641.

15. For a detailed discussion and analysis of the fitting parameters: see the Supporting Information.

16. Herbert DE, Lionetti D, Rittle J, Agapie T. J Am Chem Soc. 2013; 135:19075–19078. [PubMed: 24304416]

17. The oxidation of 2 is actually not observed in CH_2Cl_2 within the potential window of 0–1.0 V (vs. Fc/Fc^+).

18. Unlike the study reported by Que and co-workers (Ref. [6]), this study does not address the reactivity differences of high-valent terminal Mn^{IV}-oxo species. The observed differences in this study are due to different rates of Mn^{IV}-oxo formation, generated by oxygen atom transfer from ^sPhIO to 1 or 2, which is the rate limiting step. High-valent Mn^{IV}-oxo formation was not observed, most likely due to a fast C–H oxygenation step.

19. a) Neu HM, Baglia RA, Goldberg DP. Acc Chem Res. 2015; 48:2754–2764. [PubMed: 26352344] b) Hong S, Wang B, Seo MS, Lee Y-M, Kim MJ, Kim HR, Ogura T, Garcia-Serres R, Clémancey M, Latour J-M, Nam W. Angew Chem Int Ed. 2014; 53:6388–6392.Angew Chem. 2014; 126:6506–6510.c) Collman JP, Chien AS, Eberspacher TA, Brauman JI. J Am Chem Soc. 2000; 122:11098–11100.d) Jin N, Groves JT. J Am Chem Soc. 1999; 121:2923–2924.

Figure 1.
General molecular structure of $[LFe_3(PhPz)_3OMn]^{n+}$ 3 ($n = 2$–3; top left), supported by pyrazolates and a 1,3,5- triarylbenzene-based ligand. The inset shows the coloring scheme for the metal oxidation states.
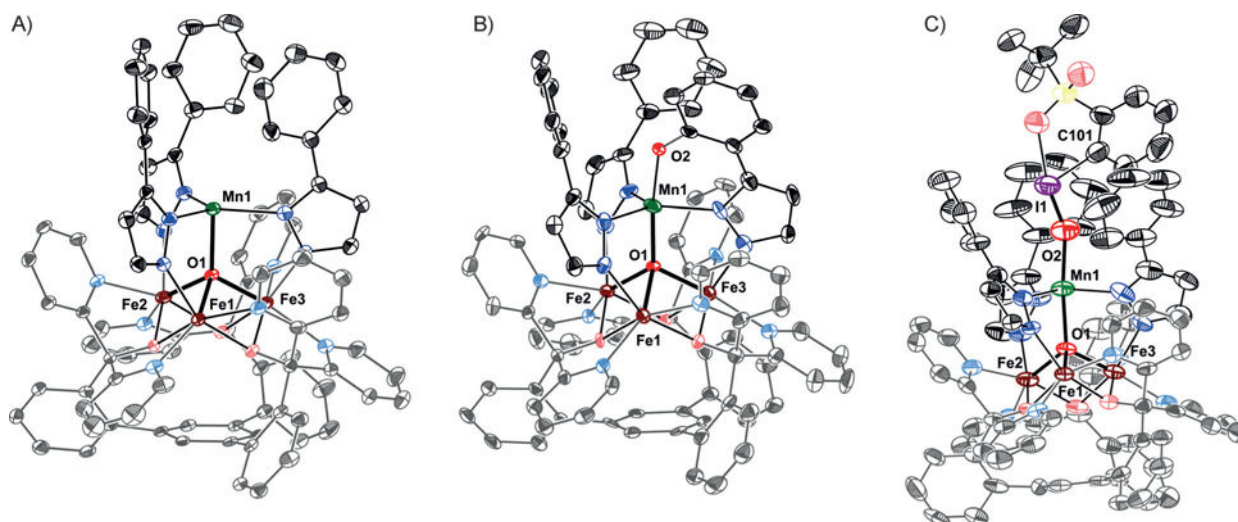
Figure 2.
Crystals structures of A) [LFe$_3$(PhPz)$_3$OMn][OTf]$_2$ (**1**); B) [LFe$_3$(PhPz)$_2$(OArPz)OMn]
[OTf]$_2$ (**5**); and C) [LFe$_3$(PhPz)$_3$OMn(^{s}PhIO)][OTf]$_3$ (**4**). Thermal ellipsoids are shown at
the 50% probability level. Hydrogen atoms, outer-sphere counter ions, and co-crystallized
solvent molecules are not shown for clarity. See Table S1 for a summary of selected bond
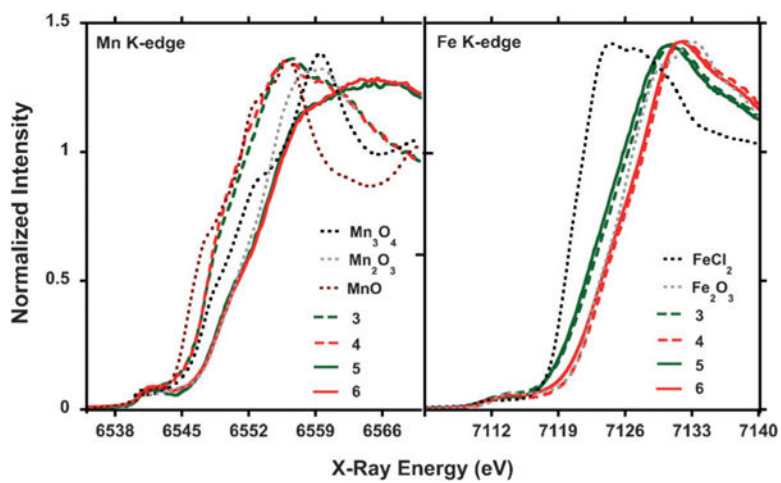lengths and angles.

Figure 3.
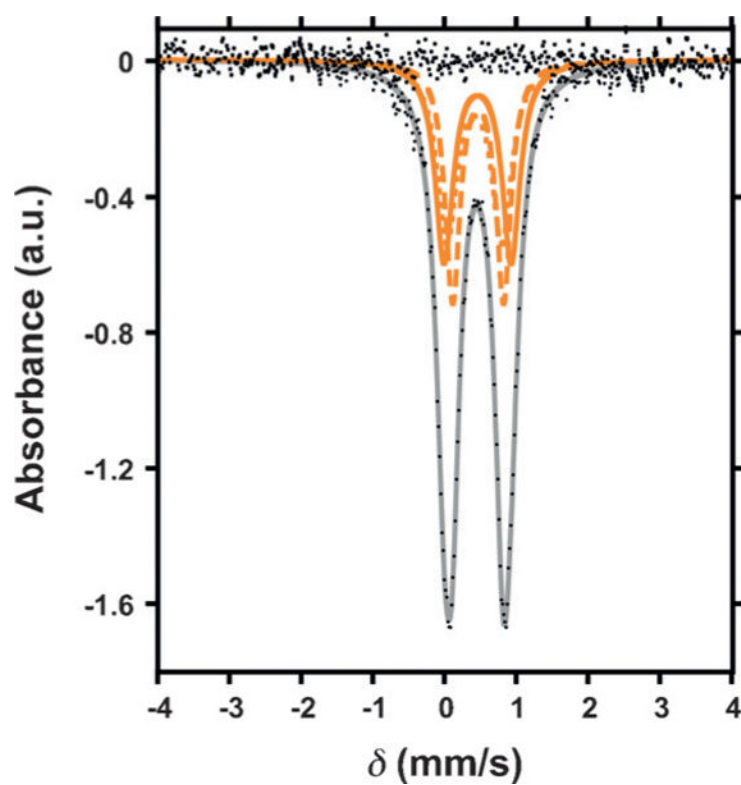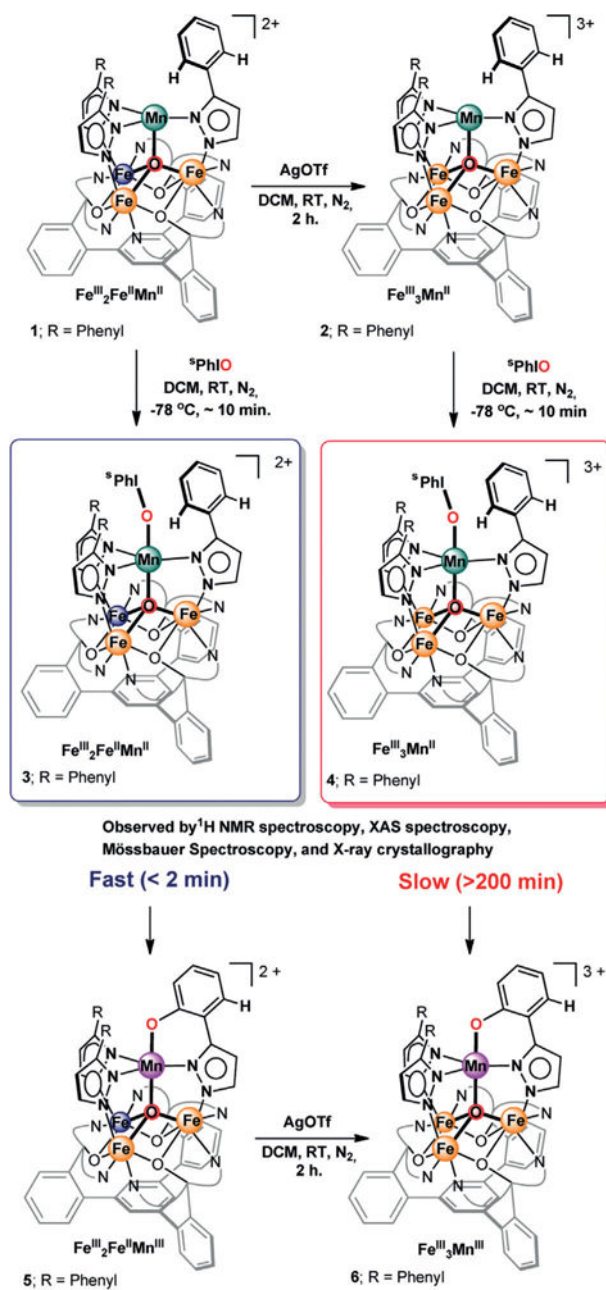Normalized Mn and Fe K-edge XANES spectra (10 K) of compounds **3**–**6**, compared to MnO, Mn_2O_3, Mn_3O_4 or to $FeCl_2$, and Fe_2O_3.

Figure 4.
Zero-field ^{57}Fe Mössbauer spectrum (80 K) of [LFe$_3$(PhPz)$_3$OMn(^{s}PhIO)][OTf]$_3$ (**4**).

Scheme 1.
Synthesis of triiron manganese clusters **1**–**6**.